Modelling-based assessment of suspended sediment dynamics in a hypertidal estuarine channel.

Laurent O. Amoudry · Rafael

Ramirez-Mendoza · Alejandro J. Souza ·

Jennifer M. Brown

Laurent O. Amoudry

National Oceanography Centre

Joseph Proudman Building

6, Brownlow Street, Liverpool, L3 5DA, UK

Tel.: +44-151-795-4914

Fax: +44-151-795-4801

E-mail: laou@noc.ac.uk

Rafael Ramirez-Mendoza

National Oceanography Centre

E-mail: rrmenz@noc.ac.uk

Alejandro J. Souza

National Oceanography Centre

E-mail: ajso@noc.ac.uk

Jennifer M. Brown

National Oceanography Centre

E-mail: jebro@noc.ac.uk

Abstract We investigate the dynamics of suspended sediment transport in a hyper-tidal estuarine channel which displays a vertically sheared exchange flow. We apply a three-dimensional process-based model coupling hydrodynamics, turbulence, and sediment transport to the Dee Estuary, in the north-west region of the UK. The numerical model is used to reproduce observations of suspended sediment and to assess physical processes responsible for the observed suspended sediment concentration patterns. The study period focuses on a calm period during which wave-current interactions can reasonably be neglected. Good agreement between model and observations has been obtained. A series of numerical experiments aims to isolate specific processes and confirm that the suspended sediment dynamics result primarily from advection of a longitudinal gradient in concentration during our study period, combined with resuspension and vertical exchange processes. Horizontal advection of sediment presents a strong semi-diurnal variability, while vertical exchange processes (including time-varying settling as a proxy for flocculation) exhibit a quarter-diurnal variability. Sediment input from the river is found to have very little importance and spatial gradients in suspended concentration are generated by spatial heterogeneity in bed sediment characteristics and spatial variations in turbulence and bed shear stress.

Keywords Suspended sediment · Modelling · Dee Estuary · tidal advection

1 Introduction

Estuaries are highly dynamic environments that are characterized by complex and competing physical processes both in terms of hydrodynamics and in terms of sediment dynamics. Suspended particulate matter is closely linked to estuarine turbidity; it impacts water quality and estuarine ecology; and it also contributes to the overall

estuarine sediment budgets. Temporal variations in suspended sediment concentrations and their correlation with tidal currents are thus critical towards understanding and predicting net transport, pathways, and estuary health.

Observations combined with modelling approaches have enabled the explanation of complex suspended sediment temporal patterns. In particular, observed suspended sediment concentrations have been interpreted as the result from the combined effect of tidal resuspension and tidal advection of a horizontal concentration gradient in tidally dominated coastal and shelf seas (e.g., Weeks et al, 1993; Jones et al, 1996; Jago and Jones, 1998; Bass et al, 2002). In regions where the largest tidal constituent is M2, tidal resuspension produces peaks with M4 variability while advection of horizontal gradients produces peaks with M2 variability, which can combine and result in the so-called twin-peak feature (Weeks et al, 1993). While the earlier studies previously mentioned were based on simplified modelling approaches, with inherent limits in terms of general validity (e.g., Jago and Jones, 1998; Jago et al, 2006), this fundamental concept has since been reported in three-dimensional numerical results: e.g., Souza et al (2007) in the North Sea; and Stanev et al (2007) in the East Frisian Wadden Sea, which is a shallow and strongly non-linear tidal system.

In estuaries, the confluence and mixing of fresh riverine water and salty oceanic water leads to several additional baroclinic physical mechanisms which may impact suspended sediment dynamics. The presence of density gradients results in significantly more complex systems. In particular, tidal straining (e.g., Simpson et al, 1990), asymmetry in mixing (e.g., Jay and Musiak, 1994), damping of turbulence by stratification (Geyer, 1993), and longitudinal density gradients (Burchard et al, 2008) have all been shown to impact suspended sediment dynamics and contribute to residual sediment transport. Tidal variations in particle size can also occur and modify temporal pat-

terns in suspended sediment (e.g., Jago et al, 2006). In turn, variations in settling rates and flocculation may introduce phase lags between the suspended sediment and underlying current, and change the overall net transport (e.g., Winterwerp, 2011). Most of these estuarine physical processes have not been considered in combination with the conceptual model of Weeks et al (1993), and interpretation of complex, including twin-peak, suspended sediment patterns is still incomplete in tidally dominated estuaries where longitudinal gradients in sediment may occur.

Modelling systems employed to investigate sediment transport in estuaries increasingly rely on three-dimensional baroclinic models (e.g. Burchard et al, 2004; Park et al, 2008; de Nijs and Pietrzak, 2012; Ralston et al, 2012). From a physical process point-of-view, process-based modelling is extremely valuable towards isolating and assessing specific processes, either via the invasive numerical approach of switching on or off given processes, or via selective analysis of individual contributions from numerical simulations with high predictive skill (e.g. Burchard and Hetland, 2010). From a modelling point-of-view, even though three-dimensional baroclinic models are demanding both in terms of computational power and quantity of input data, they are necessary to fully represent estuarine dynamics. Less complex approaches fundamentally rely on simplifying assumptions and may not be able to represent all required processes. For example, depth-averaged modelling cannot reproduce all baroclinic processes (e.g., Souza and Lane, 2013), and local one-dimensional vertical models commonly assume simple behaviour of horizontal (density) gradients (e.g., Simpson and Souza, 1995; Burchard and Hetland, 2010).

In the current study, we present a three-dimensional baroclinic process-based modelling system, which is applied to a hypertidal region of freshwater influence and estuaries therein. Several recent observational campaigns have focused on the same study area

and have thus provided data for model validation. We focus on one specific estuary in which complex temporal patterns are observed for suspended sediment concentration, including the so-called twin-peak feature. We will use the process-based model in order to assess how the interplay between vertical exchange processes and tidal advection of spatial gradients can explain the observed suspended sediment behaviour. Results from this study will also provide some insight on a priori requirements for good predictive ability at intratidal timescales, in turn important for predictions of net transport.

We focus our study in the Dee Estuary, which is located in the south-east corner of Liverpool Bay, itself in the eastern Irish Sea. The Dee is a funnel-shaped, coastal plain estuary, which is about 30 km long with a maximum width of 8.5 km at the mouth. The main channel bifurcates forming two deep ($\approx$ 20 m) channels near the mouth which extend into Liverpool Bay: the Hilbre Channel in the east and the Welsh Channel in the west. The mean annual river discharge is about 31 m^3/s and peak flow can reach 300 m^3/s at the Manley Hall gauging station. The mean spring tidal range at the mouth is approximately 10 m, tidal currents can reach over 1 m/s in the channels, and the tide is close to a standing wave. The large tidal range results in significant intertidal areas, which contribute further to the complexity of the physical processes.

Although the Dee imports sediment, a hypsometrical analysis suggests that it may be approaching equilibrium with an associated decrease in accretion rates (Moore et al, 2009). However, more detailed studies are still required to better understand the sediment transport patterns and budgets. Bolaños et al (2013) assessed the relative contributions of several physical processes to the overall circulation in the Dee Estuary. They showed that the two channels present distinctive tidally-averaged estuarine circulation behaviours, which are unaffected by stormy periods (Brown et al, subm) (this issue): the Hilbre Channel has a vertically sheared exchange flow pattern, while the

Welsh Channel has a horizontally sheared exchange flow pattern. Even though the Dee Estuary presents an interesting challenge due to the complexity of physical process interactions, process-studies of sediment transport in the Dee, either via observations or modelling, are still scarce.

Within the Dee Estuary, we only focus on sediment dynamics pertaining to the Hilbre Channel. Sediment dynamics in the Welsh Channel are investigated in Ramirez-Mendoza et al (subm) (this issue). In effect, this may be viewed as a test of the relevance of the conceptual model first introduced by Weeks et al (1993) to an estuarine system in which baroclinic behaviour is significant in terms of hydrodynamics (vertically sheared exchange flow and periodic stratification) and where sediment spatial gradients are present.

We present in section 2 the field observations used in this study and the overall conditions observed during the observational campaign. The modelling system and its current implementation are presented in section 3. We then present and discuss observations (section 4) in the Hilbre Channel followed by numerical results (section 5).

2 Field observations and environmental conditions

The field observations used in this study focus on a campaign from mid February to early March 2008 during which benthic tripods where deployed at two locations, one in each estuarine channel (figure 1 panel C). We will only use in this study measurements from the mooring location in the Hilbre Channel; measurements from the Welsh Channel, which has distinctive hydrodynamics, are used in the modelling study of Ramirez-Mendoza et al (subm) (in this issue). The tripod deployed in the Hilbre

Fig. 1 Study location. A) UK coastline and boundaries of computational domains used in the nesting approach: the Irish Sea domain (dashed) and the Liverpool Bay domain (solid). B) Liverpool Bay domain and model bathymetry. C) Close-up of the mouth of the Dee, with the two channels and the locations of the moorings (black circles).

Channel is about 2.5 m high and its feet cover a circle about 3.5 m in diameter. It was equipped with different instruments to measure hydrodynamics and suspended sediment properties. A detailed description of the deployment is presented in Bolaños and Souza (2010). We will mainly use in this study data from ADCP (Acoustic Doppler Current Profiler) and LISST (Laser In Situ Scattering and Transmissometry) to provide information on flow structure and suspended sediment concentrations, although data from a near-bed ADV (Acoustic Doppler Velocimeter) are also briefly employed.

In the Hilbre Channel, the LISST100X was located 1.82 mab (metres above the bed) and was set to sample at a frequency of 0.025 Hz for 20 minutes every hour. The data have been processed using the manufacturer software and the total concentration has been calibrated using filtered water samples to obtain total sediment mass concentration values. It has to be noted that there is non negligible uncertainty in this calibration ($r^2 \approx 0.6$).

An upward looking 1.2MHz ADCP (from Teledyne RD Instruments) was mounted on top of the benthic tripod and provided data with a vertical bin resolution of 0.5 m. The ADCP provided vertical profiles of current velocities. The ADCP also recorded the acoustic backscatter strength, which can be interpreted into suspended sediment mass concentration via regression against values obtained from the water samples (e.g., Souza et al, 2004). Once again, there is non-negligible uncertainty in the quantitative mass concentration values.

Fig. 2 Conditions observed in February 2008 in the Hilbre Channel: a) water depth; b) current speed (3 metres above the bed); c) wave height; d) wave period; e) river freshwater discharge. Ebbs are highlighted by the shaded vertical bands.

Measurements of tidal current, wave properties (height and period), as well as the river discharge are presented in figure 2 for the first half of the deployment period in February 2008. Elevations and currents in the Hilbre Channel (figure 2 panels a and b) follow the dominant M2 tidal cycle with a clear spring-neap variability. The currents generally exhibit a slight flood dominance (faster peak speed during flood) due to asymmetry resulting from the generation of higher tidal harmonics in the shallow estuary. Wave observations (figure 2 panels c and d) clearly distinguish two periods. Before 21 February, waves remain small ($\leq$ 0.6 m) and short. During this period, they are unlikely to significantly contribute to sediment transport, and wave-current interactions can be neglected. After 21 February, wave height and period are larger and modulated by the tide. Full wave-current interactions should then be considered for modelling purposes. We focus our study on the calm period of current dominated conditions occurring before 21 February.

Although the river discharge (figure 2 e) remains small throughout the study, freshwater has a clear impact on the Dee hydrodynamics as periodic stratification was observed (Bolaños et al, 2013), which is consistent with values of the horizontal Richardson number (Brown et al, subm) (this issue).

3 Model description

We apply the Proudman Oceanography Laboratory Coastal Ocean Modelling System (POLCOMS) in order to reproduce the observed hydrodynamic and sediment

behaviour in the Dee Estuary. Even though this modelling system does include a wave

model, we focus on a calm period and do not account for wave-current interactions. We

will test and implement the model under several approaches and assumptions, which

will be introduced in section 5.1.

3.1 Hydrodynamic model

The POLCOMS is based on a three-dimensional baroclinic numerical model formulated

in spherical polar terrain-following coordinates (Holt and James, 2001). The hydrody-

namic model solves the three-dimensional, hydrostatic, Boussinesq equations of motion

separated into depth-varying and depth-independent parts to allow time splitting be-

tween barotropic and baroclinic components. The detailed governing equations have

been presented in Holt and James (2001) and are not repeated here.

Turbulent stresses and fluxes are modelled following turbulent viscosity and turbu-

lent gradient diffusion hypotheses. In turn, eddy viscosity and diffusivities are obtained

via coupling to the General Ocean Turbulence Model (GOTM, Umlauf et al (2005))

presented in Holt and Umlauf (2008). In the present study, we employ the $k - \varepsilon$ model

with stability functions derived from the second-order model of Canuto et al (2001).

The bottom shear stress is calculated using a drag coefficient expression that relies on

a logarithmic near-bed velocity profile.

3.2 Suspended sediment transport model

The suspended sediment transport model allows the use of an unlimited number of

sediment classes. Each class is specified by user-defined values for sediment settling

velocity, critical shear stress for erosion, and erosion rate. Bed processes characteristic of cohesive sediments, such as bed consolidation, are neglected in this study.

For each class k, the suspended sediment concentration c_k follows an advection-diffusion equation

$$\frac{Dc_k}{Dt} = T(c_k) + \frac{W_{s,k}}{H}\frac{\partial c_k}{\partial \sigma} + S_{c,k} \tag{1}$$

where $S_{c,k}$ is an optional sediment source/sink term, $W_{s,k}$ the settling velocity for class k. $T(c_k)$ represents transport of sediment via turbulence diffusion; it is closed using the turbulence model and assumes that the sediment diffusivity is equal to the buoyancy diffusivity. The left hand side term represents the material derivative and, as such, includes advection of sediment. Horizontal diffusion is neglected.

At the free surface, the vertical flux of sediment is set to vanish. At the bottom boundary (sediment bed), the vertical flux of sediment is taken to be equal to the sum of erosion E and deposition D. This condition is implemented by including erosion and deposition as a source/sink term for the bottom grid of the water column and preventing advective and diffusive fluxes into the bed. Deposition is due to gravitational settling and is considered to occur for all bed shear stresses

$$D_k = W_{s,k}c_k \tag{2}$$

The erosion flux is directly related to the excess bed shear stress via a linear dependence: (e.g., Ariathurai, 1974; Amoudry and Souza, 2011):

$$E_k = E_{0,k}(1 - \phi)\left(\frac{\tau_b}{\tau_{ce,k}} - 1\right) \tag{3}$$

where $E_{0,k}$ is the user-defined erosion rate for class k, ϕ is the top bed layer porosity, τ_b the bed shear stress magnitude, and $\tau_{ce,k}$ the critical stress value for erosion for class k.

3.3 Model setup

The overall hydrodynamic setup used to model the Dee Estuary follows that of Bolaños et al (2013). The numerical domain extends over the Liverpool Bay region at a resolution of about 180 m (figure 1). The bathymetry consists of digitized hydrographic charts combined with LIDAR and multibeam data. Three-dimensional baroclinic effects, river inputs, surface heating and offshore density structure are all considered. Liverpool Bay is subjected to a hypertidal regime (spring tidal range in excess of 10 m) and intertidal areas are significant. Wetting and drying algorithms are therefore also implemented. The bed roughness is taken to be constant and uniform across the Liverpool Bay domain, and its value is $z_0 = 0.003$ m.

3.3.1 River inputs

Freshwater river flow is numerically implemented by increasing the total water elevation by an amount calculated from the river volume flux at the river source location. This also results in generation of momentum via the introduction of a local free-surface gradient. The salinity is then adjusted throughout the water column assuming that the river flow is fresh. By default, the temperature of the river input is taken to be in equilibrium with the ocean temperature. Even though this may not be perfectly accurate, a difference in temperature between river and ocean would remain small in February and would have a negligible impact on the density structure in the estuary compared with the effect of salinity. River sediment load can be included via the source term in equation 1 at the river source location. It adds sediment by specifying its concentration within the volume of freshwater representing river input. Daily averaged river discharges from the Environmental Agency river gauge network are made available

from the Centre of Ecology and Hydrology (CEH) to drive the freshwater input. Data on the river sediment load is not available and, when taken into account, the river sediment concentration is taken as a user-defined constant value.

3.3.2 Boundary and initial conditions

A nesting approach is employed to prescribe offshore boundary conditions for elevations, currents, temperature and salinity. Boundary values are obtained from numerical simulations for the entire Irish Sea (see figure 1) and are then used to force the three-dimensional hydrodynamics in the Liverpool Bay domain. Atmospheric forcing consists of hourly wind velocity and atmospheric pressure, and three-hourly cloud cover, humidity and air temperature.

The model hydrodynamics are spun up from rest for the month of January, with initial salinity and temperature being respectively set at 35 PSU and 7°C. Sediment transport is initialized from clear waters on 1 February 2008, as it was found that this is sufficient to spin up suspended sediment concentrations before the observational period, which starts on 12 February 2008. Data on the initial bed sediment distribution are not available. Several conditions have been implemented depending on the modelling approach selected and will be discussed in section 5.1.

4 Observed sediment dynamics

Observations alone may result in better understanding of the physical processes responsible for the overall Dee sediment dynamics, which may then help inform modelling studies. LISST-measured total suspended sediment concentrations (SSC) are presented in figure 3 for approximately a spring-neap cycle. Even though waves may influence

Fig. 3 Suspended sediment concentrations measured by the LISST in the Hilbre Channel (bottom panel). Top panel: Depth-averaged along channel velocity (DAV_{alg} in red) and water level (ζ in black). Ebbs are marked by the shaded vertical bands, floods by the unshaded bands.

the system after 21 February, twin-peaks in SSC can be repeatedly distinguished in the time history. These specific patterns are particularly clear at the start of the record around 15-16 February, then 19 to 22 February, and around 25-26 February. These twin-peaks are also present in other SSC observations in the Hilbre Channel (for example in February 2006 as reported in Thurston (2009)). Such repetition hints that this pattern is the result of common and important mechanisms in the Dee Estuary.

More detailed observations from both the LISST and ADCP are presented in figure 4 for our specific period of interest, i.e. the modelled period. We only present observations of total measured suspended sediment concentrations (SSC) and emphasize that quantitative agreement has to be considered as speculative given the uncertainties introduced by the respective conversions into mass concentrations. Nevertheless, the temporal patterns remain unaffected by uncertainties introduced by the conversion into mass concentration. The measurements display variable correlation between the two instruments and the observed behaviour is clearly more complicated than simple resuspension. Under this unique process, we would expect SSC peaks to correlate with velocity peaks with a phase lag due to the time needed for vertical transport of suspended particles (e.g., Souza et al, 2004). The ADCP-inferred SSC after 19/20 February indeed seems to support such an explanation. Resuspension peaks clearly correlate with maximum currents, and the slightly stronger peaks measured by the ADCP during the last two floods are also consistent with a flood-dominant resuspension process due to the flood dominance of currents. Around neap, the ADCP peaks

do not appear to be related to maximum current, instead the temporal variation seems to become dominated by a semi-diurnal behaviour. Given that the ADCP does not provide measurements below approximately 3 mab, a plausible explanation is that re-suspension peaks at neap are not strong enough to result in sediment being lifted above the ADCP and measured. Suspended sediment measured by the ADCP would then be advected instead of locally resuspended, which is consistent with the sharp vertical front-like pattern in SSC seen around 16 and 17 February (figure 4 panel c) in a similar manner to the sediment starved case presented in Souza et al (2007).

Simple resuspension processes also cannot explain the LISST data in figure 4, which exhibits either semi-diurnal peaks or the so-called "twin-peaks" pattern over the entire calm period. A strong semi-diurnal variability in SSC is typically explained by advective processes in tidally-dominated environments (e.g., Weeks et al, 1993; Jones et al, 1996; Jago and Jones, 1998; Bass et al, 2002), twin-peaks resulting from the superposition of tidal resuspension on these advective processes. In the Dee Estuary, the situation is unfortunately complicated by the presence of a number of processes related to baroclinic behaviour, periodic stratification, mixed sediments and it is not evident whether the same conceptual explanation remains valid.

We believe that the significant difference in the qualitative temporal patterns mea-sured via ADCP or LISST primarily results from limitations inherent to acoustic mea-surements of sediments in mixed sediment estuarine environments. Acoustic techniques are indeed limited in terms of measuring across an entire sediment size distribution, in particular at the extremes (e.g., Lynch et al, 1994). These techniques are also greatly affected by flocculation processes (MacDonald et al, 2013). We will thus mainly focus on model-observation comparison against the LISST data in the following sections.

Fig. 4 Measured suspended sediment concentrations (SSC) in the Hilbre Channel: a) Water elevation (shaded area) and depth-averaged along-channel current (black line and symbols), b) Total SSC measured by the LISST at 1.82 mab (black) and for the bottom ADCP bin (red), c) vertical profile of suspended sediment concentration inferred from the ADCP data. Numbers on the time axis correspond to days in February 2008 (each at 00:00).

Even though we will investigate the importance of vertical exchange processes and horizontal advection via model simulations, it is still interesting to evaluate the relative importance of advective transport and vertical turbulent diffusion on the suspended sediment. In particular, we can scale these terms as they appear in the suspended sediment mass balance (equation 1). We then obtain that the ratio of advective transport to vertical turbulent diffusion scales as:

$$\frac{ADV}{DIF} = \frac{UH^2}{LK_z} \tag{4}$$

where U is a current velocity scale, H a vertical length scale (e.g., depth of estuary), L a horizontal length scale, and K_z the sediment diffusivity. This ratio is equivalent to an estuarine Péclet number. Taking the following values for the Hilbre Channel $U = 0.5$ m/s, $H = 10$ m, $L = 10$ km, $K_z = 0.01$ m^2 s^{-1} results in a ratio of 0.5, indicating that advective transport is hardly negligible. While the chosen values are somewhat arbitrary, they are consistent with values from Bolaños et al (2013) and they all tend to underestimate the calculated ratio and the importance of advection.

5 Numerical results

5.1 Numerical experiments

The hydrodynamic and sediment model is implemented under several approaches and assumptions. The aim is to assess the relative importance of vertical exchange processes

16

Table 1 Numerical experiments summary.

Simulation name	Sediment classes	Initial bed composition	River sediment input
1Sm	1 ($Ws = 0.6$ mm/s)	Uniform	No
1Sf	1 ($Ws = 0.1$ mm/s)	Uniform	No
1Sc	1 ($Ws = 1.0$ mm/s)	Uniform	No
1Sv	1 (variable W_s)	Uniform	No
3S	3	Following figure 5	No
3Suni	3	Uniform	No
3Sri	3	Following figure 5	Yes

and of tidal advection of spatial gradients towards reproducing and explaining the observed temporal SSC behaviour. The numerical simulations employed in the present study are summarized in table 1. We consider either a single sediment class (*1S* in the simulation name) or a multiclass approach with three classes (*3S* in the simulation name). For the monoclass approach, several constant settling velocities have been tested (denoted by suffixes *f*, *m*, *c* representing fine, medium, and coarse sediments). One monoclass simulation (denoted by the suffix *v*) uses an empirical formulation for prescribing a time-varying settling rate. For the multiclass simulations, river sediment input has been considered (denoted by suffix *ri*), and two initial bed compositions implemented: one spatially uniform (suffix *uni*), and one spatially varying (no suffix). It has to be noted that the monoclass simulations implicitly employ uniform initial bed distributions.

Sediment model parameters are summarized in table 2 for both monoclass and multiclass approaches. A default constant value for the settling velocity ($W_s = 0.6$ mm/s) has been estimated from the size distribution which has been measured by the LISST and averaged over the modelled period (i.e., 14 to 21 February). Both

Table 2 Sediment model parameters for monoclass and multiclass modelling. (τ represents the turbulent stress)

Number of classes	W_s (mm/s)	E_0 (kg m^{-2} s^{-1})	τ_{ce} (Pa)	Source
1	0.1; 0.6; 1.0	1.25 $\times 10^{-5}$	0.19	Bed
	$W_s(\tau)$	1.25 $\times 10^{-5}$	0.19	Bed
3	0.1	1.25 $\times 10^{-5}$	0.05	Bed (+ River)
	0.6	1.25 $\times 10^{-5}$	0.19	Bed
	1.0	1.25 $\times 10^{-5}$	0.5	Bed

smaller and larger settling rates are also investigated. The time-varying settling rate is implemented as an empirical formula which relates W_s to the turbulent stress in order to represent processes inducing temporal changes in settling rate, such as aggregation at slack water (e.g., Thurston, 2009) and turbulence induced break-up. This empirical formula is derived from the data collected in the Dee during the same deployment and follows the approach of Ramirez-Mendoza et al (subm) (this issue). More details are provided there and not repeated here. The multiclass approach only considers sediment parameters constant in time for each sediment class.

Different mechanisms are considered for the generation of longitudinal concentration gradients. Simulations using spatially uniform bed characteristics do not exclude this, as spatially varying erosion can still be induced by spatial variations to the bed shear stress. In the multiclass simulations, additional mechanisms are considered via the specification of a spatially varying initial bed composition and river sediment input. The initial bed is chosen to consist of three types of sediment with different constant settling rates and different constant critical stress for erosion. Data on spatial variations in bed composition in the Dee Estuary are unfortunately not available, even though grab samples within the channels indicate a bed composed of muddy sand. Instead, we

Fig. 5 Initial composition of sediment bed in the Dee for simulations with three sediment classes. The colours correspond to the percentage of the given sediment class initially present in the bed. The classes each have a different settling velocity: from left to right $W_s = 0.1$ mm/s, $W_s = 0.6$ mm/s, and $W_s = 1.0$ mm/s.

have to rely on a more conceptual and qualitative approach. Our starting point is well-known sorting mechanisms due to tidal forcing that result in finer sediment landward (e.g. van Straaten and Kuenen, 1958; Holland and Elmore, 2008). We therefore choose to introduce an initial condition that prescribes changes to the distribution of sediment based on the local bathymetry. For depths higher than the mean sea level, the bed is initially composed of 50% fine ($W_s = 0.1$ mm/s) and 50% medium ($W_s = 0.6$ mm/s) for depths larger than 10 metres the bed is initially composed of 25% medium and 75% coarse ($W_s = 1.0$ mm/s), in between the bed is composed of 50% medium and 50% coarse. The resulting composition is presented in figure 5. Even though the specific numbers are somewhat arbitrary, this composition is consistent, at least conceptually and/or qualitatively, with current general understanding of sediment heterogeneity in tidal flats (e.g., Holland and Elmore, 2008). A spatially uniform composition of 50% medium, 25% fine and 25% coarse is also implemented in order to isolate the effect of spatial gradients in bed composition.

River input of sediment is considered in one simulation. As mentioned previously, this is implemented by specifying a constant sediment concentration value (of fine particles only) to the freshwater input.

5.2 Hydrodynamic model validation

Model results and observations are compared during the calm period 14 to 21 February. This is done using the numerical results from the nearest neighbouring computational grid point to the mooring location. Differences between the four computational points surrounding the deployment are not found to be significant, and we do not believe that more complicated interpolation would impact the results. In addition to model-observation comparison plots, we will quantify the skill of the model by applying the following statistical parameters to the sediment concentration time history at 1.82 mab in comparison with the LISST data: relative bias, index of agreement (d) following Willmott et al (1985), and r^2, which describes the proportion of the total variance explained by the model. Relative bias and index of agreement d are respectively defined as:

$$Rel.Bias = \frac{\sum_{i=1}^{N}(M_i - O_i)}{\sum_{i=1}^{N}|O_i|} \tag{5}$$

$$d = 1 - \frac{\sum_{i=1}^{N}(M_i - O_i)}{\sum_{i=1}^{N}\left[|M_i - \bar{O}| + |O_i - \bar{O}|\right]^2} \tag{6}$$

where M represents model results and O observations, the overbar denotes the mean value. The relative bias expresses the under or over prediction of the model with respect to the observations. Values less than 0.1 are judged as excellent and less than 0.2 as very good. The index of agreement measures the skill of the model with values of 1 for perfect agreement and 0 for complete disagreement.

Even though the hydrodynamic component of the model has been investigated in Bolaños et al (2013) and found to reproduce reasonably well the observations in the Dee, we present in figure 6 the comparison between depth-varying ADCP data and model results for the along-channel velocity at the deployment location in the Hilbre Channel.

Fig. 6 Model-observation comparison for the along-channel velocity component. a) water elevation ζ with observations in black circles and model results in the red line; b) Depth-averaged along channel velocity component (positive for flood) again with observations in black circles and model results in the red line; c) along-channel depth-dependent velocity measured by ADCP; d) along-channel depth-dependent velocity predicted by model. Numbers on the time axis correspond to days in February 2008 (each at 00:00).

The comparison is good and leads to high indices of agreement for both the elevations and along-channel velocities (respectively 0.99 and 0.98, the later value applying to both the depth-averaged velocity or depth-dependent velocity). Even though the across-channel component is not predicted as well, it is much smaller (Bolaños et al, 2013) and only has a second-order effect on sediment dynamics. The same hydrodynamic model has also been validated against observations at other locations in Liverpool Bay (e.g., Brown et al, 2011, 2013). Altogether, this confirms the good predictive capability of this model in terms of hydrodynamics.

Predictions of sediment resuspension critically depend on the model's ability to correctly reproduce near-bed shear. We present in figure 7 model-observation comparison using measurements by an ADV mounted under the benthic tripod and located at 1 mab. The comparison for speed, which thus includes both along-channel and across-channel components, is shown in panel b. The model reproduces the timing of maximum speed well. Some effects of the benthic tripod on hydrodynamics were observed during this deployment (Bolaños et al, 2011), and may explain the underprediction of the ADV-measured speed by the model. Measured and modelled turbulent stresses, in order to represent vertical mixing, are compared in panel c. The model predicts the timing of large stresses well, even though some discrepancies exist for the stress magnitude especially during flood. These may reflect some model shortcoming,

Fig. 7 Near-bed model-observation comparison. a) Depth-averaged along channel current from ADCP (black circles) and model (red line); and water elevation (shaded area). b) Speed measured by an near-bed ADV (black line with pluses) and predicted speed (red line). c) Turbulent stress derived from the ADV measurements (black line with pluses) and modelled turbulent stress (red line). d) Turbulent kinetic energy (TKE) derived from ADV (black line with pluses) and modelled friction velocity u_f (red dashed line).

but may also be due to some effect of the tripod on the measured turbulent stresses (e.g., Bolaños et al, 2011). Finally, the turbulent kinetic energy calculated from the ADV measurements is presented alongside the model friction velocity in panel d, as further illustration of the good temporal behaviour of the model. Even though the turbulent kinetic energy and the friction velocity are not the same quantity they are related as the second is the bed boundary condition for the first.

As mentioned previously, we will focus on comparisons of SSC at the deployment location using the LISST data at 1.82 mab. The present sediment transport model, based on POLCOMS coupled to GOTM, has already been shown to have good predictive power for simple suspended sediment dynamics (Amoudry and Souza, 2011). Combined with the good predictive power of both hydrodynamics (figure 6) and near-bed shear (figure 7), we thus have confidence in its ability to reproduce the fundamental processes of advective transport, vertical turbulent diffusion and settling. The statistical parameters for all numerical simulations are summarized in table 3. They have been calculated from hourly time series over 7 days. Due to the unperfect correlation between mass and volume concentrations in the data analysis, both bias and index of agreement may be partly attributable to uncertainties in the experimental data. This would be less the case for r^2 for which agreement on periodicity and phase of temporal patterns would be important.

Table 3 Summary of model skill for sediment concentration.

Numerical simulation	Rel. Bias	d	r^2
1Sm	-0.35	0.55	0.15
1Sf	3.86	0.37	0.64
1Sc	-0.69	0.45	0.03
1Sv	-0.14	0.54	0.06
3S	-0.15	0.86	0.59
3Suni	5.22	0.29	0.60
3Sri	-0.15	0.86	0.59

Fig. 8 Sensitivity of model results to sediment settling velocity. Observations are plotted as circles for elevation (top panel) and as the black line with the pluses for the suspended sediment concentration (bottom panel). The model results are for one sediment class with $W_s = 0.1$ mm/s (green), $W_s = 0.6$ mm/s (red), $W_s = 1.0$ mm/s (blue). Elevations are identical for all three simulations.

5.3 One-class sediment model

Model results using the monoclass approach are compared with the LISST data in figures 8 and 9. The default simulation (*1Sm* in table 3 plotted in red in both figures) does not reproduce the data well. Some important physical processes are therefore not properly taken into account. Changes to the settling rates are presented in both figures (different constant values in figure 8 and variable settling in figure 9). As expected and rather obviously, the smaller the settling velocity, the larger the concentration becomes. This leads to overall bias in the numerical results, and the best agreement is found using the variable settling rate, and second best by the default constant value (table 3), both of which are really not surprising given that the settling velocity was determined based on the observations in both cases.

Fig. 9 Sensitivity of one-class model results to inclusion of empirical variations in settling rate as function of turbulent stress. Top panel: elevation in shaded area and depth-averaged along channel current. Bottom panel: suspended sediment concentrations from LISST (black line with pluses), from model with constant settling with $W_s = 0.6$ mm/s (red line) and variable settling $W_s = W_s(\tau)$ (blue line).

The more interesting behaviour concerns the temporal qualitative patterns (i.e., frequency and phase of peaks). For three simulations (*1Sm*, *1Sc*, and *1Sv*), the modelled SSC displays quarter-diurnal variability, which corresponds well to tidal resuspension and vertical exchange processes but does not reproduce the observations adequately. Most importantly, using a variable settling rate does not change the frequency and phase of SSC peaks. All three cases show low correlation to the measured SSC. The situation is clearly different for the fine particles (simulation *1Sf*): the predicted concentration time history presents distinct peaks at low water, and much increased correlation with the LISST measurements, even though the model dramatically overpredicts the amount of suspended sediment.

Such a shift in the temporal variability implies a much reduced importance of resuspension and vertical exchange processes. Instead, advection and/or dilution due to changes in water depth become dominant. The shift is due to the finest sediment displaying different dynamic suspension characteristics from that of the other two. In particular, it remains in suspension for significantly longer periods of time, as shown by the following values for the ratio between a settling time scale and the tide period: $H/(W_s T) = 2.23$, 0.37, 0.22 for $H = 10$ m, T the M2 tidal period, and increasing W_s values. The major shift in dynamical behaviour of suspended material is also depicted by a change of about one order of magnitude for the ratio of settling to turbulent suspension time scales (e.g., Prandle, 1997). Even under stratified conditions, for which

turbulent mixing can be suppressed, the dynamical behaviour of suspended material is drastically modified for extremely fine particles (e.g., Geyer, 1993). Altogether these promote the relative contributions of advection and dilution, both of which exhibit semi-diurnal variations.

5.4 Multiclass sediment model

Conceptually, we expect the non-uniform bed composition to lead to strong horizontal gradients in suspended sediment, which will then be advected by the tidal currents. These gradients can first be set up via two principle mechanisms: spatial heterogeneity in sediment resuspension or river source of sediment. Both are considered and their relative importance in the Dee is investigated. For the bed composition specified and illustrated in figure 5, we expect the model to produce high sediment concentrations dominated by fines in the upper estuary and low concentrations offshore. Following the conceptual model of Weeks et al (1993), such a gradient would then be advected along the estuary and result in a strong semi-diurnal component to the temporal SSC patterns, as shown by simple numerical models (e.g., Jones et al, 1996). It has to be noted that spatial heterogeneity in sediment resuspension can also be induced by spatial differences in levels of turbulence and bed shear stress. As mentioned previously, this is implicitly taken into account in all simulations presented.

Figure 10 presents the model-observation comparison for the concentration time history at 1.82 mab in the Hilbre Channel. As conceptually expected and explained, the results from simulation $3S$ are in much better agreement with the LISST data. The statistical parameters in table 3 are also greatly improved. Numerical results that include a riverine source of fine sediment to the $3S$ simulation ($C_r = 100$ g/m^3 in

Fig. 10 Model-observations comparison for suspended sediment concentration (SSC) for the three-class simulations with initial bed composition given by figure 5 in red and uniform initial bed composition in blue. The observations are in black.

simulation 3Sri) are indistinguishable from those without riverine sediment input (i.e., model-model comparison between simulations *3S* and *3Sri*). While the actual value for C_r is arbitrary since no data is available, significant changes to the SSC at the measurement location are only obtained in the model with unrealistically and unphysically large value (i.e. $C_r \approx 10^4$ to 10^5 g/m^3). These numerical results strongly suggest that river sediment input does not directly contribute to the observed SSC patterns in a significant manner.

Changing the initial bed composition leads to dramatic changes. The modelled suspended sediment concentration severely overpredicts the LISST observations when a uniform initial bed is implemented (figure 10). The numerical results from simulation *3Suni* are actually quite similar to those of simulation *1Sf*, and sediment transport is then dominated by the dynamical behaviour of the fine class. It is clear that the horizontal gradients introduced via the non-uniform initial distribution are key to the overall sediment transport dynamics in the Dee Estuary. In comparison, horizontal gradients induced by gradients in turbulence and bed shear stress are not sufficient to reproduce the observed patterns.

Figure 11 separates the three classes and their individual contribution to the overall SSC signal. The semi-diurnal peaks mostly consist of the fine sediment ($W_s = 0.1$ mm/s). This is particularly instructive as this sediment type is initially not present at the measurement location and the only mechanism that can therefore explain the peaks of fine sediment is horizontal advection. The two remaining classes, and in particular

Fig. 11 Contribution of the three sediment classes to the SSC pattern at 1.82 mab in the Hilbre Channel. Top panel: water elevation as the shaded area, and depth-averaged along channel current (model in red and ADCP data in black circles). Bottom panel: SSC from LISST as the black line, SSC for the slow-settling sediment in magenta, SSC for the medium-settling sediment class in cyan, and SSC for the large-settling sediment class in red (mostly trace amounts compared with the other two classes).

the medium sediment ($W_s = 0.6$ mm/s) class, present temporal variations that are suggestive of resuspension as they correlate well with maximum current and maximum stress. It is important to note that the semi-diurnal peaks of fine sediment happen around slack water, the net flux of fine sediment is thus uncertain from such short simulations. This makes any inference on sediment budgets, which would require results for long-term spatial patterns, difficult.

The numerical results do provide information on the vertical structure of the suspended sediment. Figure 12 presents the vertical profiles at the deployment location for the study period for each of the three sediment classes included. Even though it may be tempting to compare in details these results to the ADCP measurements (presented in figure 4), we already discussed the limitations and shortcomings of the ADCP-derived SSC in the present situation. The different behaviour of the three classes is once again evident. The slow-settling sediment is advected in a well-mixed vertical structure past the deployment location due to the action of tides and exhibits a distinct semi-diurnal variability. The other two classes present behaviours linked to resuspension processes, as shown by the correlation to peak currents, and exhibit asymmetric quarter-diurnal variability. A number of barotropic and baroclinic processes, one of which is asymmetry of the barotropic tide and related turbulence, combine to produce this asymmetry and it is not our aim to identify and further separate these processes. Overall, figure

Fig. 12 Suspended sediment profiles. a) Water elevation as the shaded area, and depth-averaged along channel current (model in red and ADCP data in black circles); Modelled SSC vertical profiles (simulation *3S*) for the three sediment classes: b) $W_s = 1.0$ mm/s; c) $W_s = 0.6$ mm/s; d) $W_s = 0.1$ mm/s.

12 provides another illustration of the conceptual model following which a longitudinal gradient in suspended concentration generates pulses of high sediment tidally advected first offshore then landwards past the stationary deployment (panel d), to which resuspension dominated patterns (panel c) are superposed. Depending on the relative importance of the two contributions, semi-diurnal peaks, or twin-peaks, or even quarter-diurnal peaks (not observed and reproduced in the present study) may be obtained.

6 Concluding remarks

We have combined numerical results from a sediment transport model with field observations in order to investigate sediment dynamics in the Hilbre Channel of the Dee Estuary, UK. Baroclinic behaviour is important both in the channel studied, which exhibits a vertically-sheared exchange flow and periodic stratification (Bolaños et al, 2013), and in Liverpool Bay, which is a region of freshwater influence.

Observations of suspended sediment concentration using optical techniques (a LISST) display semi-diurnal peaks or twin-peaks close to low water. Although intermittent in time, this is observed repeatedly and is an important manifestation of sediment dynamics in the Hilbre Channel of the Dee Estuary. We have applied a coupled three-dimensional circulation, turbulence and sediment transport modelling system in order to reproduce and investigate the observed patterns. The model provides good predic-

tions of hydrodynamics and has shown satisfactory capabilities in terms of sediment transport.

We have used the model as an investigative tool in order to test the relevance of the conceptual model of Weeks et al (1993) to an estuarine system where baroclinic behaviour is significant and periodic stratification is observed. Numerical results have confirmed that the observed patterns of suspended sediment concentration result from superposition of tidal resuspension and tidal advection of spatial sediment concentration gradients, the second process being dominant during most of the period studied. In particular, vertical exchange processes, such as resuspension and time-varying or constant settling, have been shown to be insufficient to generate the observed strong semi-diurnal variability in suspended sediment concentration. This specific behaviour has been reproduced by the model when using the spatially heterogeous initial sediment distribution, and advection of fine particles then appears to be responsible for the observed variability in suspended concentration. Using the representative scaling introduced previously (i.e., $U = 0.5$ m/s), semi-diurnal concentration peaks due to advective processes imply a source of fine sediment about 10 km upstream of the measurement location, which corresponds well with our assumption and basic implementation of heterogeneous sediment bed.

Several mechanisms have been considered to generate the spatial concentration gradients to be advected: spatial variations in turbulence and bed shear stress (implicitly in all cases), spatial gradients in bed sediment characteristics, and river sediment inputs. Numerical results indicate how important these processes are towards reproducing observations: the first is insufficient, the second is key, the third is negligible here. In comparison, previous studies had considered general limited availability of bed material (e.g., Jones et al, 1996; Jago and Jones, 1998; Souza et al, 2007) or spatial

variations in turbulence (Stanev et al, 2007) as the mechanisms generating the concentration gradients. It has to be pointed out that the present simulations (table 1) do not allow to isolate the relative importance of spatial variations in turbulence against that of spatial gradients in bed characteristics, and removing only the first mechanism cannot easily be implemented in the full three-dimensional model. Nevertheless, being insufficient towards reproducing observations does not necessarily mean not important. In practice and in our results, horizontal concentration gradients are set up from a combination of the spatially-varying bed shear stress and spatially varying bed characteristics.

The inference from our numerical results that river sediment inputs are negligible has to be interpreted carefully as we have focused on one channel near the mouth of the estuary for a time-limited period under moderate river discharge. More impact of sediment river input is possible or likely (i) further upstream in the estuary, and (ii) under stronger river discharges. The limited period of time also means that we cannot assess whether river sediment input can generate spatial gradients in either the bed characteristics or suspended concentration over the long term. This would require numerical simulations to be undertaken over at least yearly time scales, and may provide another significant mechanism towards setting up important advective transport of sediment.

It has to be noted that the model-observation comparisons presented are mostly informative in a qualitative manner. Even though the three-dimensional baroclinic process-based model does provide a deterministic solution, several assumptions and input conditions remain somewhat conceptual in nature. This is especially true of the initial bed composition and sediment parameters for the multiclass simulations. The overall results should therefore not be considered as fully quantitative, but more qual-

itative and conceptual. Significant additional work would be necessary towards better quantitative assessments. For example, the model's sensitivity to the specification of the multiclass setup (both initial bed condition and sediment parameters) would need to be investigated further.

In spite of these limitations, this study highlights the important processes that control suspended sediment concentration in the Dee and does provide valuable insight on some modelling requirements. While high quality input data should be considered as an obvious generic requirement, the present numerical results suggest a few more detailed inferences. They confirm that knowledge of the spatial distribution of different sediment classes, each determined by settling velocity and erosion parameters (E_0 and τ_{ce} here), is very important towards accurately reproducing sediment dynamics in the Dee Estuary. However, the present work does not, and does not intend to, fully address how such spatial information can best be prescribed. Initial spatially-varying bed composition may be derived from existing data (see Nitsche et al (2007) for an example of extensive benthic mapping data), self-generated by the model (e.g., van der Wegen et al, 2011), or a combination of both (e.g., Ralston et al, 2012). Such approaches would probably result in more complex sediment distribution patterns than the ones used in this study. The reasonable results achieved here are an indication that our simple approach is sufficient to resolve the principal processes controlling sediment dynamics in the Dee Estuary during the studied period: along-estuary gradients.

References

Amoudry LO, Souza AJ (2011) Impact of sediment-induced stratification and turbulence closures on sediment transport and morphological modelling. Cont Shelf Res 31(9):912–928, DOI 10.1016/j.csr.2011.02.014, doi:10.1016/j.csr.2011.02.014

Ariathurai CR (1974) A finite element model for sediment transport in estuaries. PhD thesis, University of California, Berkeley, USA

Bass SJ, Aldridge JN, McCave IN, Vincent CE (2002) Phase relationships between fine sediment suspensions and tidal currents in coastal seas. J Geophys Res 107(C10), DOI 10.1029/2001JC001269, doi:10.1029/2001JC0012

Bolaños R, Souza A (2010) Measuring hydrodynamics and sediment transport processes in the dee estuary. Earth Syst Sci Data 2:157–165

Bolaños R, Amoudry LO, Doyle K (2011) Effects of instrumented bottom-tripods on process measurements. J Atmos Ocean Technol 28:827–837

Bolaños R, Brown JM, Amoudry LO, Souza AJ (2013) Tidal, riverine and wind influences on the circulation of a macrotidal estuary. J Phys Oceanogr 43(1):29–50, DOI 10.1175/JPO-D-11-0156.1, doi:10.1175/JPO-D-11-0156.1

Brown JM, Bolanos R, Wolf J (2011) Impact assessment of advanced coupling features in a tide-surge-wave model, polcoms-wam, in a shallow water application. Journal of Marine Systems 87:13–24

32

Brown JM, Amoudry LO, Mercier FM, Souza AJ (2013) Intercomparison of the charnock and coare bulk wind stress formulations for coastal ocean modelling. Ocean Science in press

Brown JM, Bolanos R, Souza AJ (subm) Controls on the mid-term estuarine residuals: circulation and elevation. Ocean Dynamics

Burchard H, Hetland RD (2010) Quantifying the contributions of tidal straining and gravitational circulation to residual corculation in periodically stratified tidal estuaries. J Phys Oceanogr 40:1243–1262

Burchard H, Bolding K, Villarreal MR (2004) Three-dimensional modelling of estuarine turbidity maxima in a tidal estuary. Ocean Dynamics 54(2):250–265

Burchard H, Flöser G, Staneva JV, Badewien TH, Riethüller R (2008) Impact of density gradients on net sediment transport into the Wadden Sea. J Phys Oceanogr 38:566–587

Canuto VM, Howard A, Cheng Y, Dubovikov MS (2001) Ocean turbulence. part I: One-point closure model - momentum and heat vertical diffusivities. J Phys Oceanogr 31:1413–1426

Geyer WR (1993) The importance of suppression of turbulence by stratification on the estuarine turbidity maximum. Estuaries 16(1):113–125

Holland KT, Elmore PA (2008) A review of heterogeneous sediments in coastal environments. Earth-Science Reviews 89:116–134

Holt J, Umlauf L (2008) Modelling the tidal mixing fronts and seasonal stratification of the Northwest European continental shelf. Cont Shelf Res 28:887–903

Holt JT, James ID (2001) An s coordinate density evolving model of the northwest European continental shelf 1, model description and density structure. J Geophys Res 106(C7):14,015–14,034

Jago CF, Jones SE (1998) Observation and modelling of the dynamics of benthic fluff resuspended from a sandy bed in the southern North Sea. Cont Shelf Res 18:1255–1282

Jago CF, Jones SE, Sykes P, Rippeth T (2006) Temporal variation of suspended particulate matter and turbulence in a high energy, tide-stirred, coastal sea: relative contributions of resuspension and disaggregation. Cont Shelf Res 26:2019–2028

Jay DA, Musiak JD (1994) Particle trapping in estuarine tidal flows. J Geophys Res 99(C10):20,445–20,461

Jones SE, Jago CF, Simpson JH (1996) Modelling suspended sediment dynamics in tidally stirred and periodically stratified waters: Progress and pitfalls. In: Mixing in Estuaries and Coastal Seas, Coastal and Estuarine Studies, vol 50, AGU, pp 302–324

Lynch JF, Irish J, Sherwood CR, Agrawal YC (1994) Determining suspended sediment particle size information from acoustical and optical backscatter measurements. Cont Shelf Res 14(10/11):1139–1165

MacDonald IT, Vincent CE, Thorne PD, Moate BD (2013) Acoustic scattering from a suspension of flocculatted sediments. J Geophys Res 118:2581–2594, DOI 10.1002/jgrc.20197, doi:10.1002/jgrc.20197

Moore RD, Wolf J, Souza AJ, Flint SS (2009) Morphological evolution of the Dee estuary eastern irish sea, UK: a tidal asymmetry approach. Geomorphology 103:588–596

de Nijs MAJ, Pietrzak JD (2012) Saltwater intrusion and etm dynamics in a tidally-energetic stratified estuary. Ocean Modelling 49-50:60–85

Nitsche FO, Ryan WBF, Carbotte SM, Bell RE, Slagle A, Bertinado C, Flood R, Kenna T, McHugh C (2007) Regional patterns and local variations of sediment distribution on the Hudson River Estuary. Estuarine, Coastal and Shelf Science 71(1–2):259–277

34

Park K, Wang HV, Kim SC, Oh JH (2008) A model study of the estuarine turbidity maximum along the main channel of the upper Chesapeake Bay. Estuaries and Coasts 31:115–133

Prandle D (1997) Tidal characteristics of suspended sediment concentrations. J Hydraul Eng 123(4):341–350

Ralston DK, Geyer WR, Warner JC (2012) Bathymetric controls on sediment transport in the hudson river estuary: Lateral asymmetry and frontal trapping. J Geophys Res 117(C10013), DOI 10.1029/2012JC008124, doi:10.1029/2012JC008124

Ramirez-Mendoza R, Souza AJ, Amoudry LO (subm) Modelling flocculation in a hypertidal estuary. Ocean Dynamics

Simpson JH, Souza AJ (1995) Semidiurnal switching of stratification in the region of fresh-water influnce of the Rhine. J Geophys Res 100(C4):7037–7044

Simpson JH, Brown J, Matthews J, Allen G (1990) Tidal straining, density currents, and stirring in the control of estuarine stratification. Estuaries 13(2):125–132

Souza AJ, Lane A (2013) Effects of freshwater inflow on sediment transport. Journal of Operational Oceanography

Souza AJ, Alvarez LG, Dickey TD (2004) Tidally induced turbulence and suspended sediment. Geophys Res Lett 31(L20309), DOI 10.1029/2004GL021186, doi:10.1029/2004GL021186

Souza AJ, Holt JT, Proctor R (2007) Modelling SPM on the NW European shelf seas. In: Coastal and Shelf Sediment Transport, Geological Society of London, pp 147–158

Stanev EV, Brink-Spalink G, Wolff JO (2007) Sediment dynamics in tidally dominated environments controlled by transport and turbulence: A case study for the East Frisian Wadden Sea. J Geophys Res 112(C04018), DOI 10.1029/2005JC003045, doi:10.1029/2005JC003045

van Straaten LMJU, Kuenen PH (1958) Tidal action as a cause of clay accumulation. Journal of Sedimentary Petrology 28(4):406–413

Thurston W (2009) Turbulence as a mediator of processes in a macrotidal estuary. PhD thesis, University of Leeds

Umlauf L, Bolding K, Burchard H (2005) GOTM - Scientific Documentsion. Version 3.2. Marine Science Reports 63, Leibniz-Institute for Baltic Sea Research, Warnemünde, Germany

Weeks AR, Simpson JH, Bowers D (1993) The relationship between concentrations of suspended particulate material and tidal processsses in the Irish Sea. Cont Shelf Res 13(12):1325–1334

van der Wegen M, Dastgheib A, Jaffe BE, Roelvink D (2011) Bed composition generation for morphodynamic modeling: case study of San Pablo Bay in California, USA. Ocean Dynamics 61(2–3):173–186

Willmott CJ, Ackleson SG, Davis RE, Feddema JJ, Klink KM, Legates DR, O'Donnell J, Rowe CM (1985) Statistics for the evaluation and comparison of models. J Geophys Res 90(C5):8995–9005

Winterwerp JC (2011) Fine sediment transport by tidal asymmetry in the high-concentrated Ems River: indications for a regime shift in response to channel deepening. Ocean Dynamics 61:203–215, DOI 10.1007/s10236-010-0332-0, doi:10.1007/s10236-010-0332-0

Figure 1

Figure 2

1
2
3
4
5
6
7
8
9
10
11
12
13
14
15
16
17
18
19
20
21
22
23
24
25
26
27
28
29
30
31
32
33
34
35
36
37
38
39
40
41
42
43
44
45
46
47
48
49
50
51
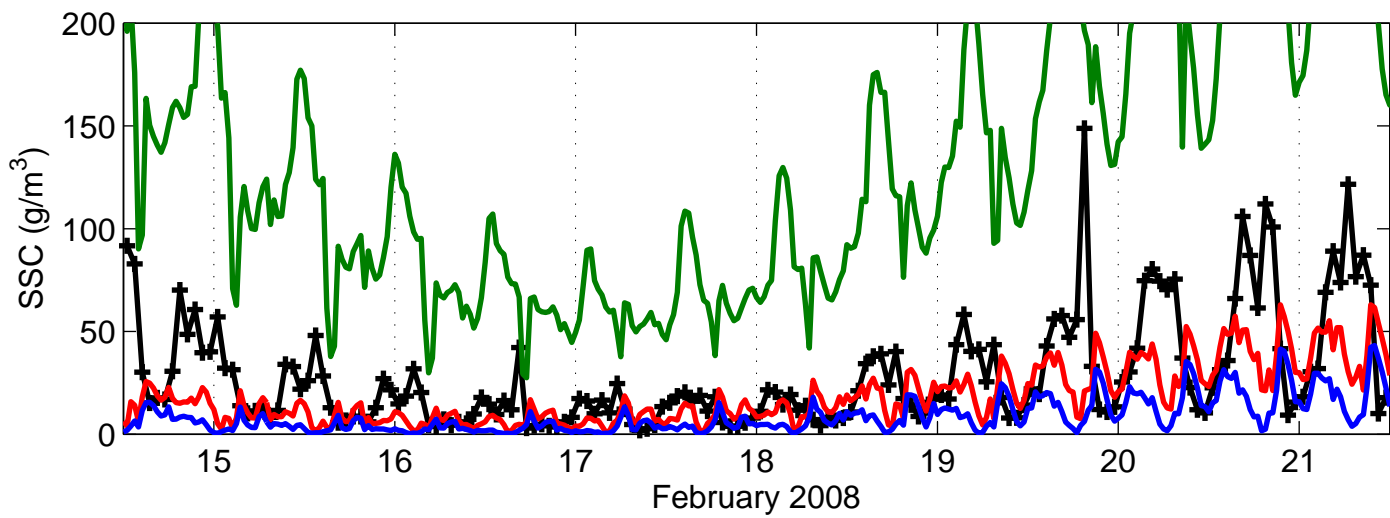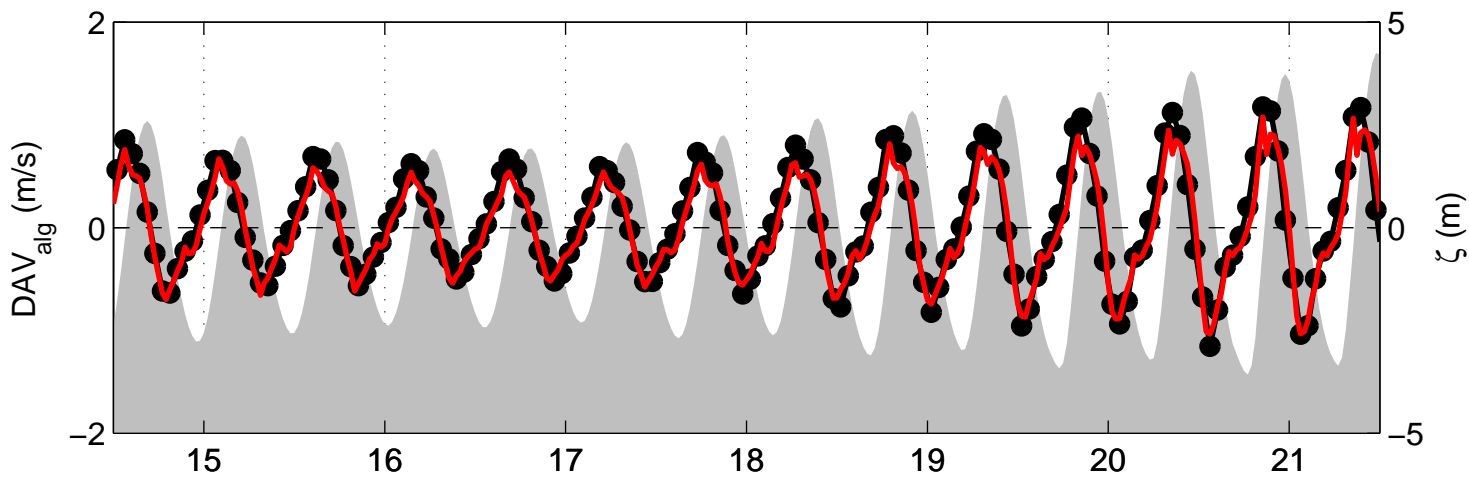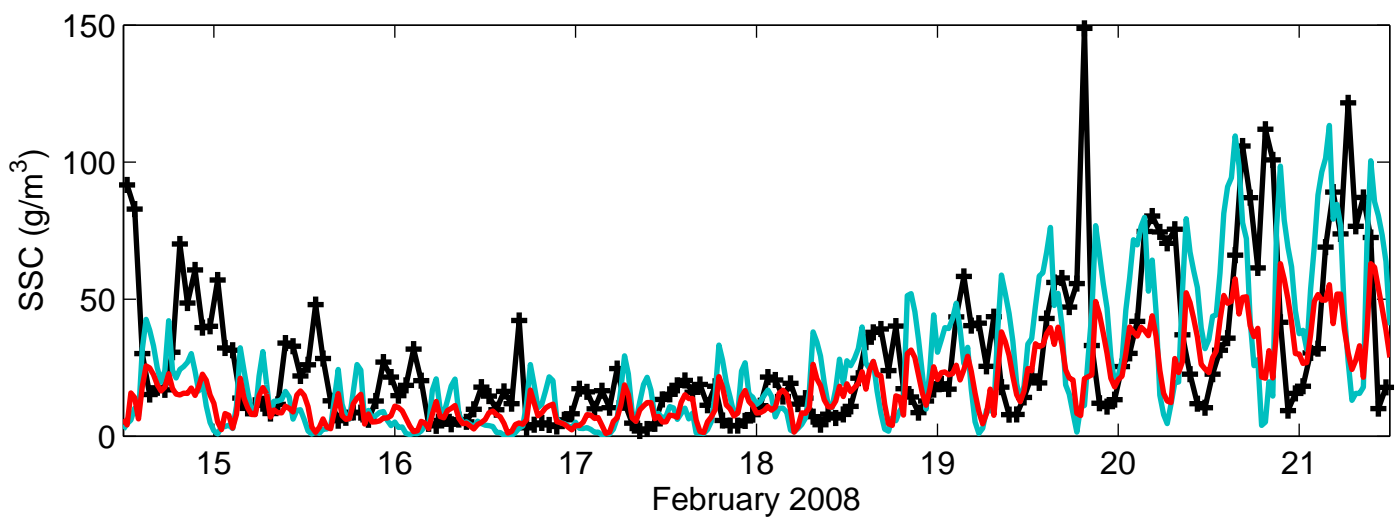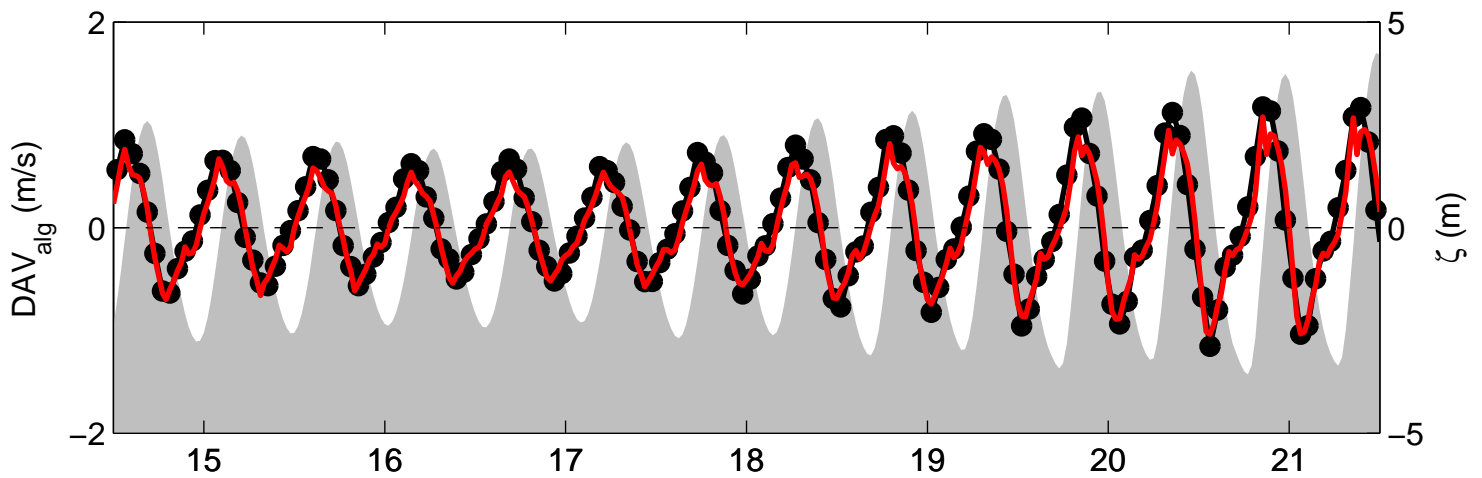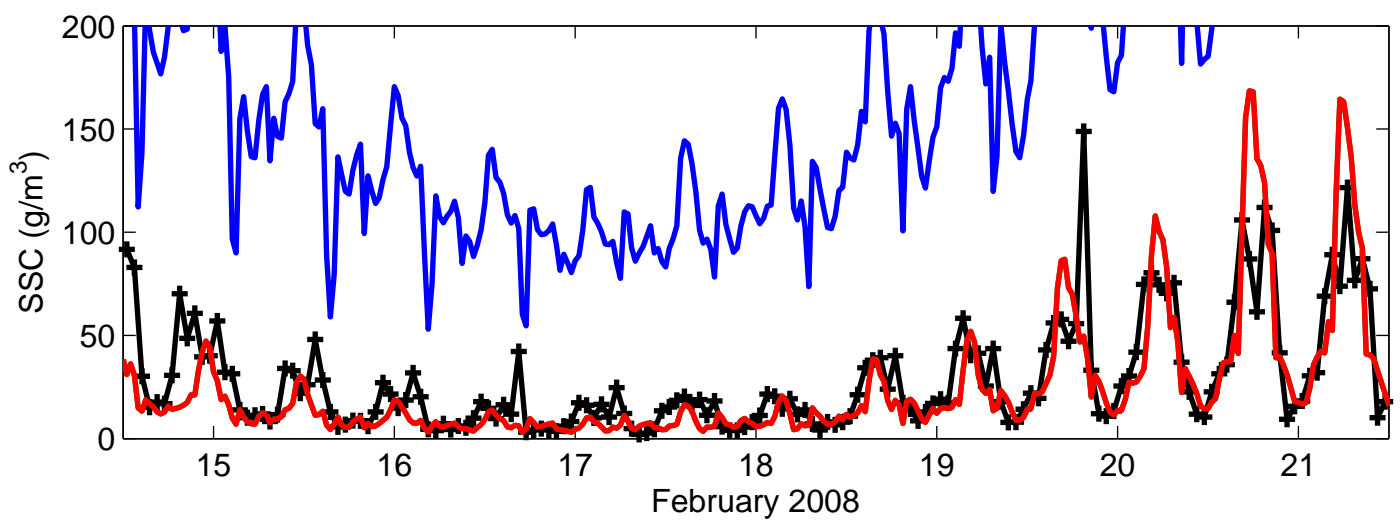52
53
54
55
56
57
58
59
60
61
62
63
64
65

Figure 3
Click here to download Manuscript: SPM_lisst_SN.eps
Click here to view linked References

February 2008

Figure 4

Figure 5
Click here to download high resolution image
Click here to view linked References

Figure 6

Figure 7

1
2
3
4
5
6
7
8
9
10
11
12
13
14
15
16
17
18
19
20
21
22
23
24
25
26
27
28
29
30
31
32
33
34
35
36
37
38
39
40
41
42
43
44
45
46
47
48
49
50
51
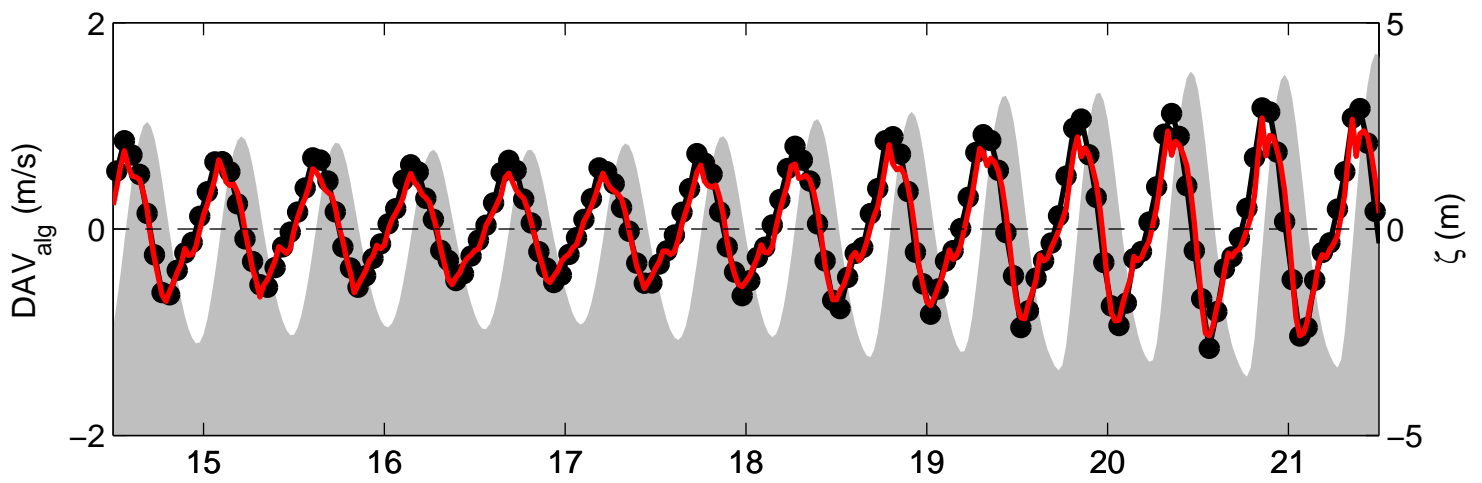52
53
54
55
56
57
58
59
60
61
62
63
64
65

Figure 8
Click here to download Manuscript: SPM_2pans_1SWs.eps
Click here to view linked References

1
2
3
4
5
6
7
8
9
10
11
12
13
14
15
16
17
18
19
20
21
22
23
24
25
26
27
28
29
30
31
32
33
34
35
36
37
38
39
40
41
42
43
44
45
46
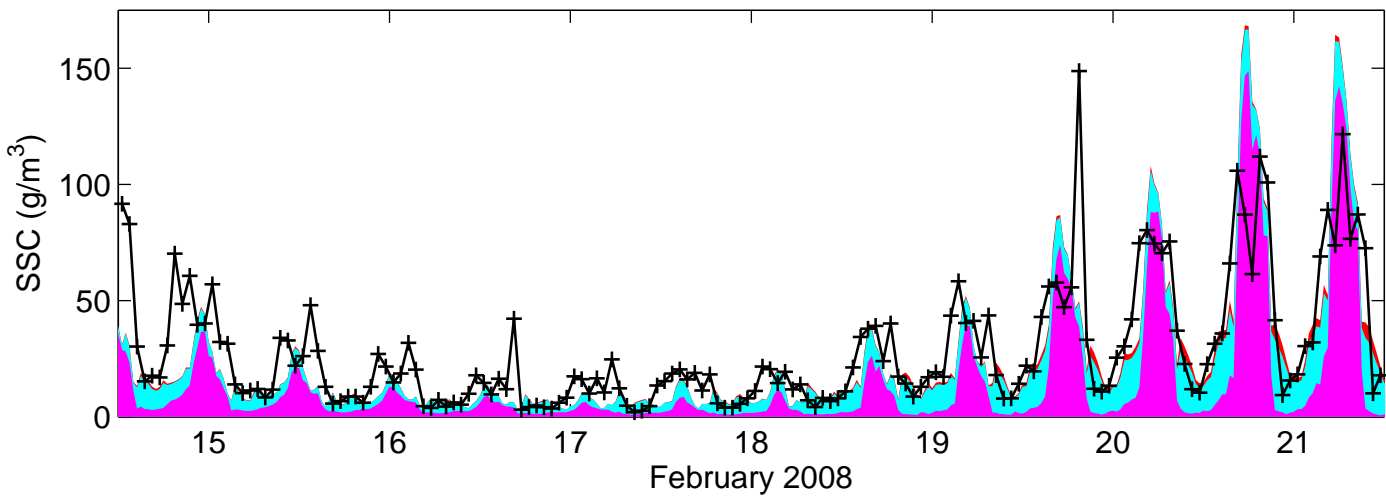47
48
49
50
51
52
53
54
55
56
57
58
59
60
61
62
63
64
65

Figure 9

Figure 10

1
2
3
4
5
6
7
8
9
10
11
12
13
14
15
16
17
18
19
20
21
22
23
24
25
26
27
28
29
30
31
32
33
34
35
36
37
38
39
40
41
42
43
44
45
46
47
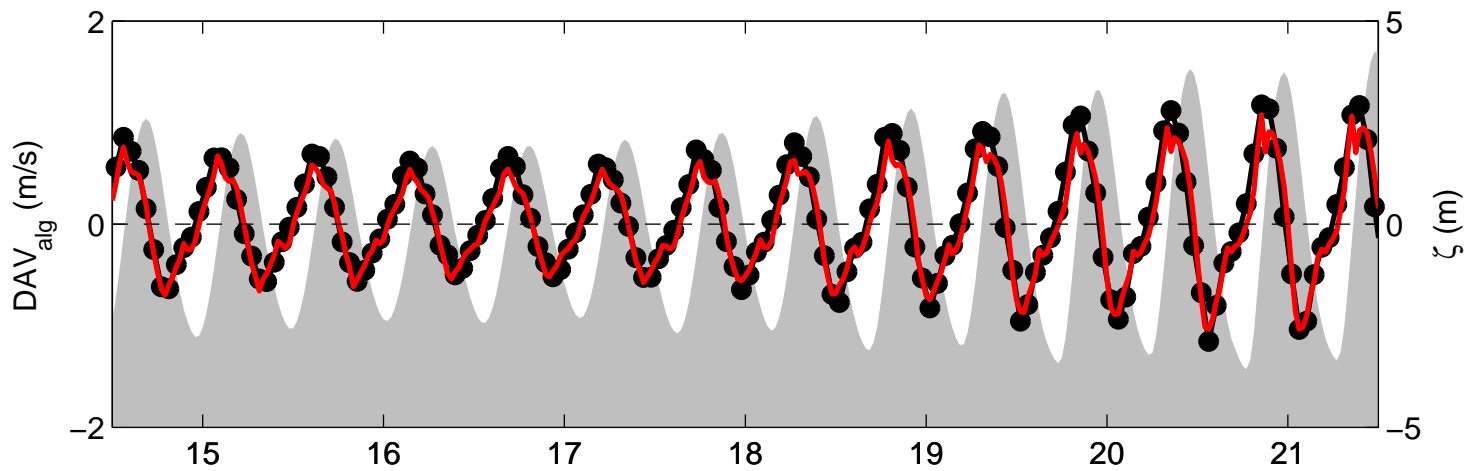48
49
50
51
52
53
54
55
56
57
58
59
60
61
62
63
64
65

Figure 11

1
2
3
4
5
6
7
8
9
10
11
12
13
14
15
16
17
18
19
20
21
22
23
24
25
26
27
28
29
30
31
32
33
34
35
36
37
38
39
40
41
42
43
44
45
46
47
48
49
50
51
52
53
54
55
56
57
58
59
60
61
62
63
64
65